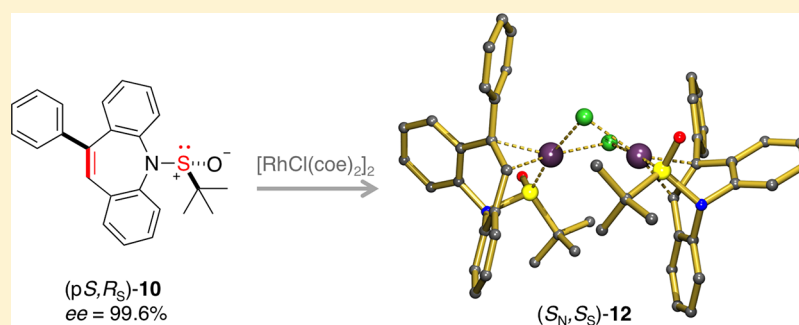


Developing Chiral Dibenzazepine-Based S(O)-Alkene Hybrid Ligands for Rh(I) Complexation: Catalysts for the Base-Free Hayashi–Miyaura Reaction

Ahmed Chelouan, Siyuan Bao, Sibylle Frieß, Alberto Herrera, Frank W. Heinemann,¹ Ana Escalona, Alexander Grasruck, and Romano Dorta*¹

Department Chemie und Pharmazie, Anorganische und Allgemeine Chemie, Friedrich–Alexander–Universität Erlangen–Nürnberg, Egerlandstraße 1, 91058 Erlangen, Germany

S Supporting Information



ABSTRACT: A stereodivergent synthesis using inexpensive reagents, i.e., dibenzazepine and glucose-derived *t*-Bu-sulfinate diastereomers (R_S)-6 or (S_S)-6, affords respective S(O)-alkene hybrid ligands (S)-7 and (R)-7 on gram scales and in excellent optical purity ($ee > 99\%$). Phenyl substitution of the dibenzoazepine backbone generates planar chirality to give epimerization-resistant (pS,R_S)-10 diastereoisomer in high isomeric purity. Furthermore, the crystal structure of widely used sulfinate (R_S)-6 is disclosed for the first time since its discovery a quarter of a century ago. Ligands 7 and 10 coordinate Rh(I) in a bidentate fashion through the S atoms and the alkene functions as evidenced by the crystal structures of complexes (R)-11 and (S_N,S_S)-12. (R)-11 catalyzes the conjugate addition of arylboronic acids to enones with enantioselectivities of up to 77% ee. The reaction proceeds smoothly also under base-free conditions at 40 °C. The planar chirality in ligand (pS,R_S)-10 is shown to override and invert the sense of chiral induction predicted by the configuration of the sulfur donor atom.

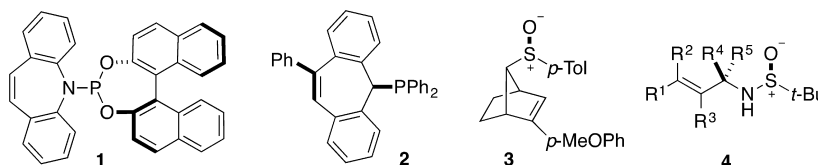
INTRODUCTION

Enantiopure sulfoxides, which are appreciated for their ease of synthesis and high stability, are important auxiliaries in asymmetric synthesis and excellent ligands for certain metal-catalyzed asymmetric organic transformations,¹ in which the polarized $R_2^+S-O^-$ function appears to induce chirality also through electrostatic effects.² Inspired by Knochel's effective norbornene-derived sulfoxide-alkene **3**³ (see Table 1) and highly flexible sulfenamido-alkene designs of type **4**⁴ and since our laboratory has been developing chiral P-alkene ligands such as **1**⁵ based on the dibenzo[*b,f*]azepine scaffold,⁶ we have been interested to extend this architecture to S(O)-dibenzazepinyl analogues⁷ by connecting the N atom with readily available chiral sulfinyl electrophiles. The alkene functions in ligands **1–4** are expected to be hemilabile thus enhancing catalyst performance. For example, complex $[Rh(\mathbf{1})_2]BF_4$ is a highly active and stereoselective catalyst for the conjugate addition of a wide range of arylboronic acids to enones.⁸ Structural studies showed that the azepine N-function in ligand **1** is hybridization-flexible in contrast to the fixed sp^3 hybridized methine in tropyliidene derivatives of type **2**. Depending on whether

the alkene coordinates to the metal or not, the N atom in **1** is sp^3 or sp^2 hybridized,⁹ a property that further “spring-loads” the alkene function toward hemilability. Here, we wish to communicate a simple procedure for the synthesis of a new class of enantiopure dibenzo[*b,f*]azepine-based S(O)-alkene ligands. We show that these diaryl, i.e., aprotic, sulfenamides¹⁰ are indeed sp^3 – sp^2 hybridization flexible at the azepine N atom while remaining stereochemically stable. Furthermore, we provide the proof-of-principle that in analogy to Grützmacher's tropyliidene-based planar-chiral architecture of ligand **2**¹¹ it is possible to generate planar chirality by introducing a phenyl group on the alkene function of the dibenzo[*b,f*]azepine backbone, and we demonstrate that these S(O)-alkenes behave as bidentate ligands for Rh(I). Rhodium complexes of chiral bis-alkene,¹² bis-sulfoxide,¹³ and in particular hybrid S(O)-alkene¹⁴ ligands are emerging as the catalysts of choice for the asymmetric conjugate addition of alkenyl and aryl boronic acids to Michael acceptors (the Hayashi–Miyaura reaction).¹⁵

Received: August 20, 2018

Table 1. Inspiring Chiral P-Alkene and S-Alkene Ligands

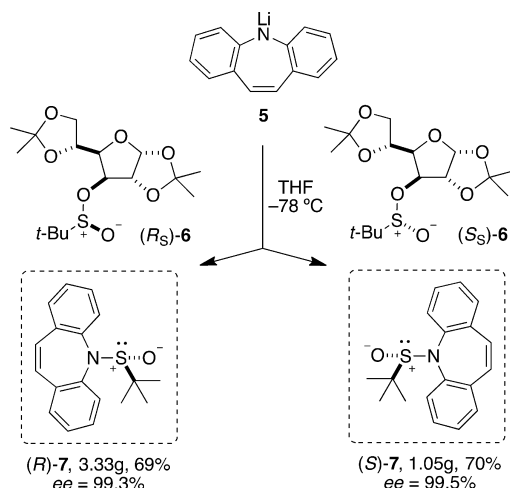


However, mild, base-free protocols for this reaction still represent a challenge,¹⁶ which the new Rh–S(O)-alkene complexes presented here partially address.

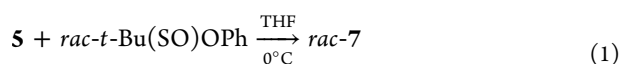
RESULTS AND DISCUSSION

Dark blue Li-amide **5**¹⁷ is quenched in THF solution at $-78\text{ }^{\circ}\text{C}$ with either diastereomers of the DAG-*tert*-butylsulfinate,¹⁸ (*R*_S)-**6** or (*S*_S)-**6**, to afford gram quantities of the (*R*)-**7** or the (*S*)-**7** enantiomer, respectively, as white powders and in excellent optical purity (see Scheme 1). It should be noted that purification

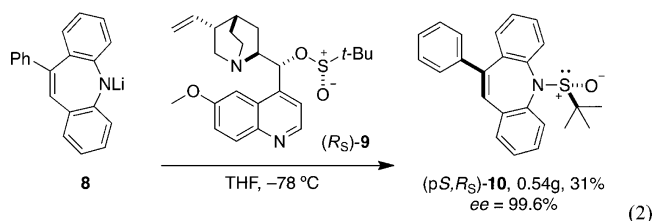
Scheme 1. Divergent Asymmetric Synthesis of the Enantiomers of S(O)-Alkene **7**



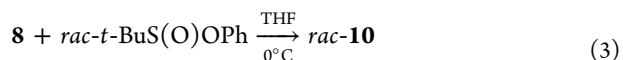
of these molecules by flash column chromatography is only possible on K_2CO_3 -impregnated silica,¹⁹ while on standard silica G60 and even in humid, air-saturated CDCl_3 solution they racemize.²⁰ In order to dispose of a standard for the determination of the optical purity of (*R*)-**7** and (*S*)-**7** by enantioselective HPLC (see Figure S4), the racemate *rac*-**7** was independently prepared by reacting racemic *t*-butyl-phenoxysulfinate with Li-amide **5** according to eq 1.²¹ Furthermore, the improved crystallinity of *rac*-**7** over its enantiopure congeners allowed us to grow X-ray quality single crystals in a 1,2-difluorobenzene/*n*-pentane solvent system, and the structure of the (*R*)-enantiomer is depicted in Figure 1. The absolute configurations of the enantiopure ligands **7** must therefore be inferred from mechanistic considerations and most probably are the ones outlined in Scheme 1.²² The stereogenic sulfur atom is pyramidal with an average bond angle of 106.7° , while the nitrogen atom is approximately trigonal planar (sp^2 -hybridized) with average bond angles of 118.9° as also observed in corresponding phosphoramidite ligands.^{5c,d,8} Similarly, the use of *rac*-**7** also helped crystallization of the corresponding rhodium complex (*vide infra*).



We recently introduced 10-phenyl-5*H*-dibenz[*b,f*]azepine for the synthesis of a P-stereogenic/planar-chiral P-alkene ligand,²³ and we found that its lithium salt **8** reacts with quinone-based sulfinate (*R*_S)-**9** at $-78\text{ }^{\circ}\text{C}$ in THF solution to afford a 2:1 diastereomeric mixture of (*pS*,*R*_S)- and (*pR*,*R*_S)-**10**.²⁴ The diastereomers are best identified by the singlet resonances of the *t*-Bu-groups in the ^1H NMR spectrum at 1.09 ppm (major) and 1.04 ppm (minor), and the major one is separated by flash column chromatography on K_2CO_3 -impregnated silica¹⁹ and isolated as a white crystalline material on a half-gram scale in excellent optical purity.²⁵ The absolute configuration (*pS*,*R*_S) is assigned by single crystal X-ray diffraction analysis (see Figure 2),²⁶ the configuration at sulfur being in accordance with the prediction based on an $\text{S}_{\text{N}}2$ type displacement reaction. As in **7**, the sp^2 N atom shows average bond angles of $118.6(14)^{\circ}$ and is slightly pyramidalized, with the tip of the N atom pointing in *endo* direction of the azepine chair. It is therefore possible, at least in the solid state, to assign the N atom the absolute configuration (*R*) instead of using the *pS* descriptor when dealing with an ideal planar N atom. On the other side, the phenyl substituted atom C8 is perfectly trigonal planar (averaged value of the three bond angles: 120.0°). No epimerization of (*pS*,*R*_S)-**10** takes place in solution under acid-free conditions, even under prolonged heating at $60\text{ }^{\circ}\text{C}$.



In a separate experiment, the racemic diastereomeric mixture of **10** was prepared according to eq 3 in analogy to *rac*-**7** (*vide supra*). The crude product of *rac*-**10** is a 1:1 diastereomeric mixture, which after recrystallization displays a 83:17 bias in favor of the (*pR*,*R*_S)/(*pS*,*S*_S)-**10** pair of enantiomers. This racemate served then as reference substance for the certification of the enantio- and diastereomeric purity of (*pS*,*R*_S)-**10**, and Figure 3 shows the chiral stationary phase HPLC traces of the reference *rac*-**10** (top) along with a diastereomerically pure sample of (*pS*,*R*_S)-**10** of medium optical purity (98% ee, bottom trace).



On a side note, DAG-sulfonates²⁸ represent an important class of chiral sulfonylating agents, and (*R*_S)-**6** is one of the most popular and practical *tert*-butyl sulfonates.²⁹ It has been discovered a quarter of a century ago,^{18a} but so far has eluded structural characterization for being described as an oil.^{18b} Structural information about DAG-sulfonates is in general scarce.^{28d} Thanks to a scaled-up procedure that affords very pure material, we were able to isolate crystalline (*R*_S)-**6**. The

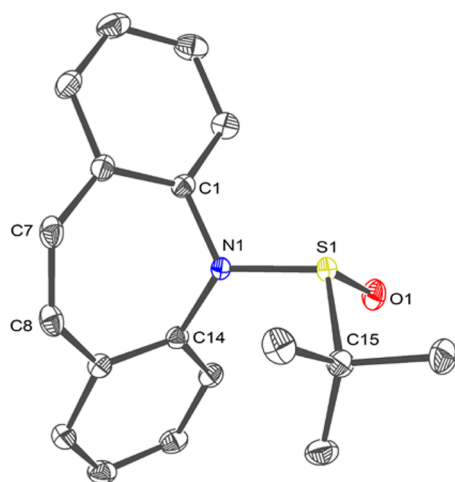


Figure 1. Molecular structure of the (*R*)-7 enantiomer in the crystal of *rac*-7 plotted with 50% displacement ellipsoids. H atoms are omitted. Selected distances (Å) and angles (deg): S1–O1 1.4884(9), N1–C1 1.4333(15), S1–N1 1.6768(10), S1–C15 1.8498(13), C7–C8 1.3432(10), O1–S1–N1 111.30(5), N1–S1–C15 103.10(5), O1–S1–C15 105.57(6), C1–N1–C14 117.17(9), C1–N1–S1 115.64(8), C14–N1–S1 123.93(8).

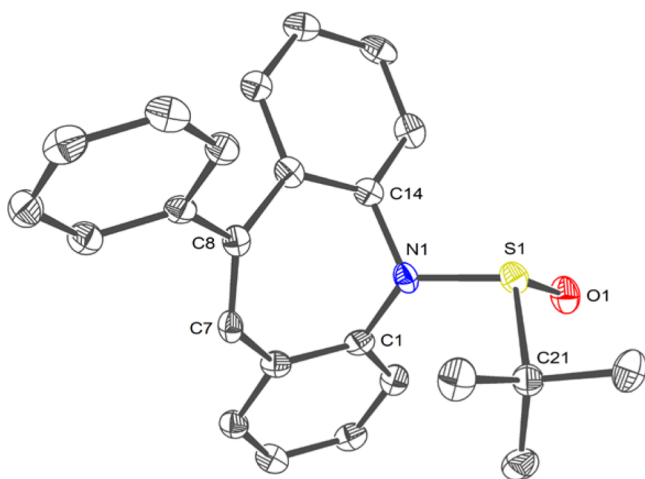
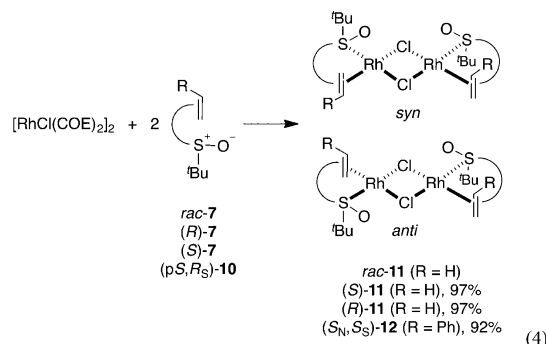


Figure 2. Molecular structure of (*pS,R_S*)-10 in the chiral crystal plotted with 50% displacement ellipsoids. H atoms are omitted. Selected distances (Å) and angles (deg): S1–O1 1.483(2), N1–C1 1.441(4), S1–N1 1.680(3), N1–C14 1.440(4), S1–C21 1.849(3), C7–C8 1.351(5), O1–S1–N1 112.47(14), N1–S1–C21 102.06(15), O1–S1–C21 105.95(15), C1–N1–S1 127.4(2), C14–N1–S1 113.6(2), C14–N1–C1 114.8(3).

structure of one of four symmetry-independent molecules is depicted in Figure 4 and confirms the expected absolute configurations of the stereogenic sulfur and carbon atoms (the other three molecules also correspond). In all four independent molecules, the *tert*-butyl and glucose moieties are turned away from each other in order to minimize steric repulsion, as indicated by the torsion angle along C1–O2–S1–C13 of -122.1° (in the other three molecules these angles measure -141.6 , -160.7 , and -169.4°) and in opposite direction when compared to the closely related (*S_S*)-DAG-cyclohexanesulfinate ($+157.2^\circ$).^{28d}

The coordination chemistry of the new ligands with Rh(I) was explored by reacting two equivalents of either (*R*)-7, (*S*)-7, or (*pS,R_S*)-10 with $[\text{RhCl}(\text{coe})_2]_2$ (coe = cyclooctene) in

benzene or toluene solution to afford optically pure dinuclear complexes (*S*)-11, (*R*)-11, and (*S_N,S_S*)-12, respectively, in high yields as yellow-orange powders (see eq 4). The complexes are soluble but unstable in chlorinated solvents and only sparingly soluble in aromatic solvents. NMR spectra of (*S*)-11 and (*R*)-11 reveal the exclusive formation of the *anti*-isomer, while (*S_N,S_S*)-12 forms a *syn/anti* mixture of 1:2. The latter can be isolated as the pure *anti*-isomer by recrystallization from benzene.



Single crystal X-ray diffraction analyses of complexes 11 and 12 were necessary to prove the proposed bidentate coordination mode of the new ligands and to gain precise structural information, not least in view of the fact that structurally authenticated chiral *S*-alkene complexes of rhodium are rare.^{4a,14a} Since crystallization of enantiopure (*S*)-11 proved problematic and did not afford diffraction-quality single crystals; racemic ligand *rac*-7 was used to synthesize complex *rac*-11 in a bid to improve crystallinity. The resulting complex exhibits NMR spectra identical to those of (*S*)-11 including the observed *anti*-selectivity, which is an indication that only homochiral dimers of *rac*-11 form. Indeed, well-shaped single crystals of *rac*-11 are readily grown from a CH_2Cl_2 /pentane mixture (see the Experimental Section), in stark contrast to the optically pure material of (*S*)-11. In contrast, X-ray quality crystals of enantiopure (*S_N,S_S*)-12 are obtained without problems by layering a C_6D_6 solution with *n*-hexane. The X-ray diffraction analyses reveal in the case of *rac*-11 a centrosymmetrical unit cell containing an enantiomeric pair of homochiral dinuclear complexes and, in the case of (*S_N,S_S*)-12, a chiral unit cell containing two independent molecules with the expected absolute configurations. The respective structures are depicted in Figures 5 and 6. Both show bidentate *S*-alkene ligands and square planar coordination geometries around the chloro-bridged Rh-centers. The Rh–Cl bonds located *trans* to the S atoms are longer than those *trans* to the alkenes by ca. 0.01–0.06 Å, and the butterfly-shaped Rh_2Cl_2 cores in *rac*-11 and (*S_N,S_S*)-12 span wing angles of 120.7 and 122.7°, respectively. Exclusive *anti*-coordination is observed in both crystals, which in the case of *rac*-11 is the consequence of a crystallographic C_2 -axis bisecting the C11–C11A and the Rh1–Rh1A vectors. The Rh–S and Rh–alkene distances compare well with values found in similar sulfoxide-alkene^{4a,14a} and *P*-alkene^{5c,8} complexes. The bite angles of ligands in the two complexes are very similar at 91.8° in *rac*-11 and 92.0° in (*S_N,S_S*)-12 (average value of four independent molecules, measured between the centroids of the alkene functions and the S atoms). The coordinated alkene bonds (C7–C8 1.423(2) in 11; C7–C8 1.427(11), C31–C32 1.436(11) in 12) are ca. 0.08 Å longer than those in respective free ligands 7 and 10 (1.3432(10) and 1.351(5) Å, see Figures 1 and 2). Furthermore, in complex 12 the C atom bearing the phenyl ring is

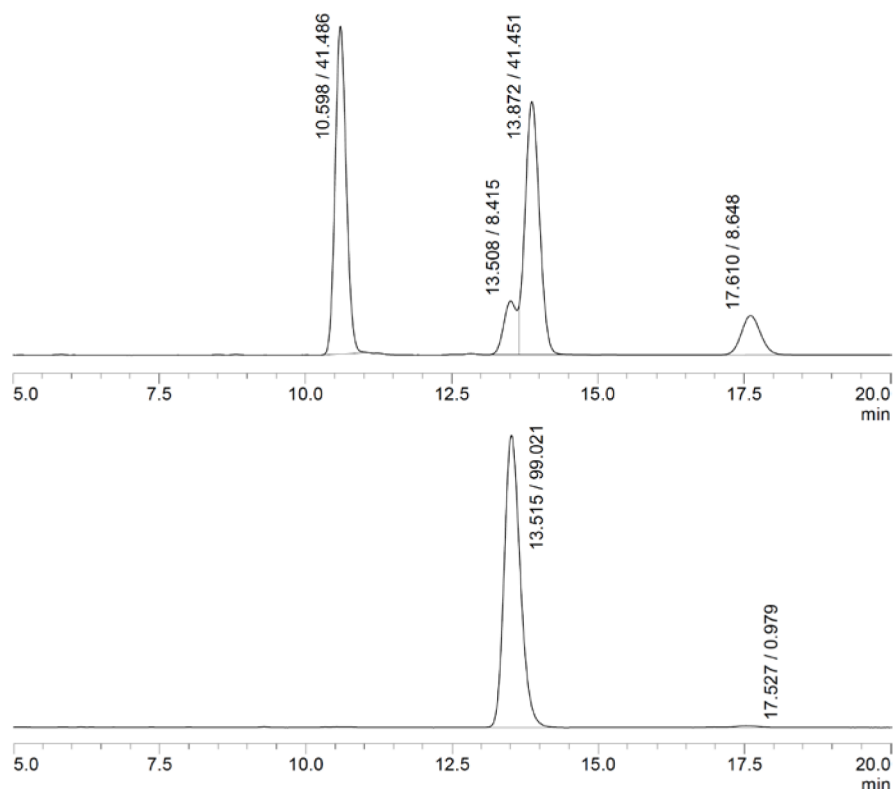


Figure 3. Chiral stationary phase HPLC traces. Top: recrystallized *rac*-**10** showing the four possible isomers with *dr* = 82.9:17.1. Bottom: sample of (*pS*,*R_S*)-**10** having *ee* = 98% for illustrative purposes.²⁷ Peak labels denote retention times and surface areas. Conditions: Chiralpak AD-H; flow rate: 1 mL/min; *n*-hexane/*i*-PrOH = 95:5.

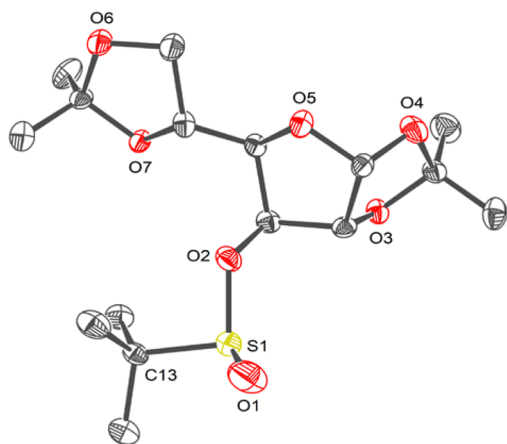


Figure 4. Structure of one out of four symmetry-independent molecules in the chiral crystal of (*R_S*)-**6** plotted with 50% displacement ellipsoids. H atoms are omitted for clarity. Selected distances (Å) and angles (deg): S1–O1 1.462(4), S1–O2 1.649(3), S1–C13 1.827(4), O1–S1–O2 106.02(19), O1–S1–C13 106.7(2), O2–S1–C13 96.87(16), C1–O2–S1 115.4(2).

slightly pyramidalized (sum of angles between C–C bonds at C14:354.2°). Alkene bond elongation and pyramidalization are the consequence of metal to alkene π -backbonding.³⁰ Furthermore, the Rh–C distance to the phenyl-substituted carbon atom is on average 5 pm longer than to the unsubstituted carbon atoms, presumably due to steric repulsion. Another important structural alteration of the coordinated ligands when compared to their free state **7** and **10** is the pronounced sp^3 character of the N atom, which may be quantified by the sum of its bond angles (336.4° in **11**; 335.8 and 334.6° for N1 and

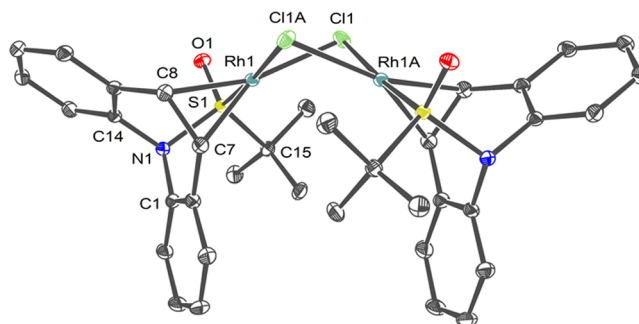


Figure 5. Molecular structure of the (*S*)-enantiomer in the racemic crystal of *rac*-**11** plotted with 50% displacement ellipsoids. H atoms are omitted. Selected distances (Å) and angles (deg): Rh1–Cl1A⁽ⁱ⁾ 2.4120 (*S*), Rh1–Cl1 2.3997(5), Rh1–S1 2.1792(5), Rh1–C7 2.1158(18), Rh1–C8 2.1394(18), C7–C8 1.423(2), S1–O1 1.4700(13), S1–N1 1.7334(15), C7–Rh1–S1 93.05(5), C8–Rh1–S1 90.51(5), Cl1–Rh1–Cl1A 81.57(2), Rh1–Cl1–Rh1A 82.305(16), S1–Rh1–Cl1 97.973(17), N1–S1–Rh1 109.55(5). Symmetry code (i): $-x + 1, y, -z + 1/2$.

N2 in **12**). We note that the N atom in complex **12** is stereogenic with (*S*)-configuration.

With well-characterized enantiopure complexes **11** and **12** in hand, their catalytic performance was benchmarked in the Hayashi–Miyaura conjugate addition of arylboronic acids **14** to enones **13** (Table 2). First, enantiomeric catalysts (*R*)-**11** and (*S*)-**11** were tested under standard biphasic dioxane/water 2:1 conditions in the presence of K_3PO_4 base at 40 °C. The respective product ketones (*R*)-**15aa** and (*S*)-**15aa** were obtained as opposite enantiomers in 75% *ee* in very close agreement, thus demonstrating stereochemical consistency

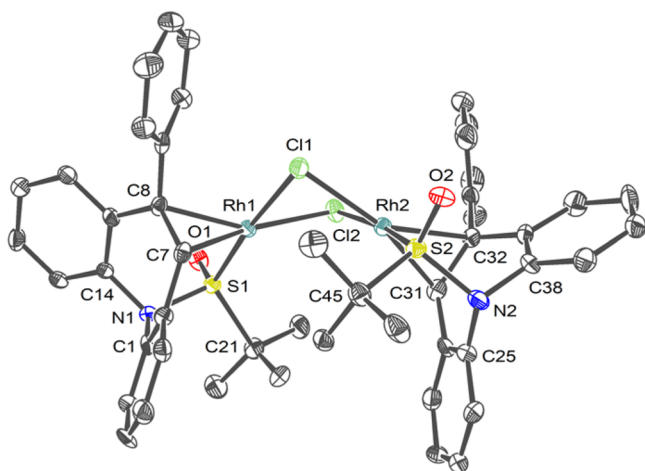
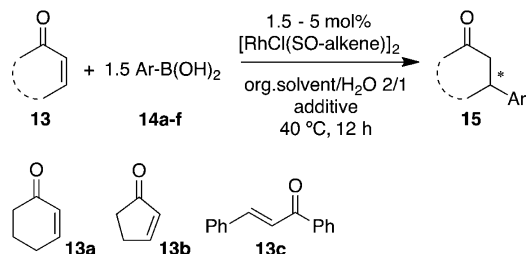


Figure 6. Molecular structure of one of two symmetry-independent molecules of *anti*-(S_N,S_S)-**12** in the chiral crystal plotted with 50% displacement ellipsoids. H atoms are omitted. Selected distances (Å) and angles (deg): Rh1–Cl1 2.400(2), Rh1–Cl2 2.382(2), Rh2–Cl1 2.370(2), Rh2–Cl2 2.4320(19), Rh1–S1 2.155(2), Rh2–S2 2.156(2), Rh1–C7 2.115(8), Rh1–C8 2.165(2), Rh2–C31 2.120(8), Rh2–C32 2.171(8), C7–C8 1.427(11), C31–C32 1.436(11), S1–O1 1.461(6), S1–N1 1.728(7), S1–C21 1.864(8), N1–C1 1.449(9), N1–C14 1.428(9), N2–C25 1.425(11), N2–C38 1.458(10), Cl1–Rh1–Cl2 79.79(7), S1–Rh1–C8 89.7(2), S1–Rh1–C7 93.4(2).

(entries 1 and 2). The use of KOH as additive led to complete erosion of enantioselectivity (entry 3) and is probably due to decomposition of the ligand. It was then found that the reaction also proceeds smoothly in the absence of base additives in a toluene/water 2:1 solvent system (entry 4). However, the base-free protocol requires higher catalyst loadings to ensure full conversion and ee values drop by 5–14% depending on the reaction (compare entries 1/4, 6/7, 8/9, and 10/11). While cyclopentenone (**13b**) gives similar results, the addition of **14a** to chalcone **13c** under base-free condition proceeds swiftly but with disappointing enantioselectivity (entry 18). Complex (S_N,S_S)-**12**, in comparison with (*R*)-**11**, returned lower chemical and optical yields in the standard reaction between **13a** and **14a** (cf. entries 4 and 5). It should be noted that even though (S_N,S_S)-**12** bears an inversely configured sulfur donor compared to (*R*)-**11** it shows the same (*R*) selectivity for the product. Clearly, the planar chirality of the alkene function in ligand (pS,R_S)-**10** (and not the chirality of the sulfur donor) controls the stereochemical outcome in this reaction, which is consistent with observations made by Knochel and co-workers³ and Liao and co-workers^{14a} with their respective planar chiral *S*(*O*)-alkene ligand systems. The stereochemical model in Figure 7 rationalizes the observed enantioselectivities for the prototypical reaction of **13a** with **14a**.³¹ In the case of catalyst (*S*)-**11** bearing ligand (*R*)-**7**, enone **13a** is oriented “up” and *anti* with respect to the bulky *tert*-butyl group, thereby presenting

Table 2. Complexes **11** and **12** Catalyze the Hayashi–Miyaura Conjugate Addition Reaction



entry	catalyst (mol %)	additive ^a	enone	boronic acid ^b	isolated yield (%)	ee (%) ^c	major isomer
1	(<i>R</i>)- 11 (1.5)	K ₃ PO ₄	13a	14a	96 (15aa)	75.2	(<i>R</i>)
2	(<i>S</i>)- 11 (1.5)	K ₃ PO ₄	13a	14a	98 (15aa)	74.9	(<i>S</i>)
3	(<i>R</i>)- 11 (5)	KOH	13a	14a	98 (15aa)	0	
4	(<i>R</i>)- 11 (5)	none	13a	14a	97 (15aa)	70	(<i>R</i>)
5	(S_N,S_S)- 12 (5)	none	13a	14a	67 (15aa)	60	(<i>R</i>)
6	(<i>S</i>)- 11 (5)	none	13a	14b	97 (15ab)	69	(<i>S</i>)
7	(<i>S</i>)- 11 (1.5)	K ₃ PO ₄	13a	14b	97 (15ab)	76	(<i>S</i>)
8	(<i>R</i>)- 11 (5)	none	13a	14c	97 (15ac)	52	(<i>R</i>)
9	(<i>R</i>)- 11 (1.5)	K ₃ PO ₄	13a	14c	98 (15ac)	66	(<i>R</i>)
10	(<i>R</i>)- 11 (5)	none	13a	14d	96 (15ad)	68	(<i>R</i>)
11	(<i>R</i>)- 11 (1.5)	K ₃ PO ₄	13a	14d	97 (15ad)	77	(<i>R</i>)
12	(<i>S</i>)- 11 (5)	none	13a	14e	95 (15ae)	70	(<i>S</i>)
13	(<i>S</i>)- 11 (5)	none	13a	14f	95 (15af)	67	(<i>S</i>)
14	(<i>S</i>)- 11 (5)	none	13a	14g	96 (15ag)	60	(<i>S</i>)
15	(<i>S</i>)- 11 (5)	none	13a	14h	97 (15ah)	40	(<i>S</i>)
16	(<i>S</i>)- 11 (5)	none	13b	14a	98 (15ba)	68	(<i>S</i>)
17	(<i>S</i>)- 11 (5)	none	13b	14b	98 (15bb)	66	(<i>S</i>)
18	(<i>S</i>)- 11 (5)	none	13c	14b	98 (15cb)	36	(<i>S</i>)
19	(S_N,S_S)- 12 (5)	none	13c	14b	traces	n.d.	

^aWith KOH additive and without additive, the organic solvent is toluene; with K₃PO₄ additive, the organic solvent is 1,4-dioxane. ^bCommercial aryl boronic acids were used as received. Ar = Ph (**14a**), 4-CH₃C₆H₄ (**14b**), 4-*t*-Bu-C₆H₄ (**14c**), 2-naphthyl (**14d**), 4-FC₆H₄ (**14e**), 4-CH₃OC₆H₄ (**14f**), 3-CH₃OC₆H₄ (**14g**), 2-CH₃OC₆H₄ (**14h**). ^cDetermined by enantioselective HPLC (see the Supporting Information); absolute configurations are assigned by comparison with reported data.

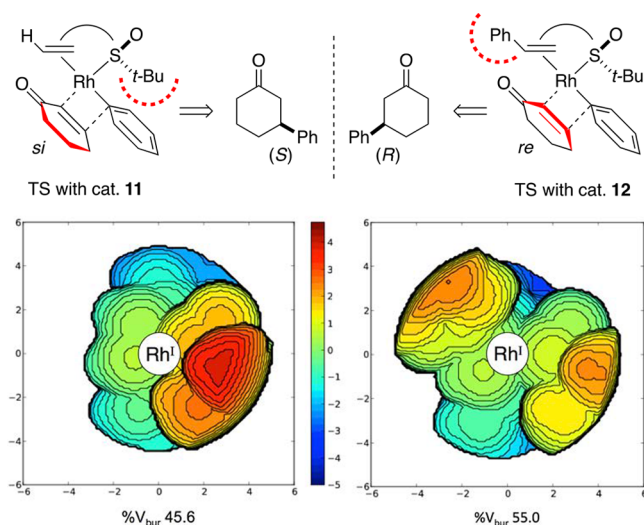


Figure 7. Top: stereochemical model (top view) for the prediction of the sense of addition of **14a** to **13a** when using catalysts **11** (left) or **12** (right). Bottom: steric maps (head-on view) of Rh(I)-coordinated ligands (*R*)-**7** (left) and (*pS,R_S*)-**10** (right) generated from crystallographic data of complexes **11** and **12** with SambVca³² freeware. Sphere radii are 5.0 Å, and bond radii are scaled at 1.17. Metal atoms and secondary ligands were excluded, and H atoms were included in the calculations. Red: more bulk; blue: less bulk.

the *si* face to the phenyl nucleophile in a [2 + 2] transition state leading to the (*S*)-configured product **15aa**. In support of this model, the head-on view of the steric map around rhodium (Figure 7, left diagram) illustrates the pronounced steric bulk of the *t*-Bu in the lower right quadrant (red and orange contours denote the methyl groups, which in solution rotate freely). In contrast, the green contours representing the coordinated ligand alkene function indicate free space for the keto function in the upper left quadrant. The inverted sense of chiral induction observed with the complex bearing ligand (*pS,R_S*)-**10** (sporting a sulfur donor with the same chirality as in (*R*)-**7**) is explained by the steric bulk of the phenyl group of the alkene donor that generates a pseudo-*C*₂ symmetric coordination environment around Rh(I) and obstructs the upper left quadrant (Figure 7, right diagram), thereby forcing coordination of the *re* side of the enone. Apparently, the planar chirality of the alkene donor is the determining stereochemical factor, overriding the opposite influence of the *tert*-butyl group of the sulfur donor. Consequently, the (*pR,R_S*)-diastereomer of ligand **10** (with the phenyl group pointing into the lower left quadrant) promises to be the better proposition for this reaction.

To conclude, we present a simple protocol that combines inexpensive dibenzazepine with readily available glucose-based sulfonates to afford optically pure *S*(O)-alkene hybrid ligands. Phenyl-substitution on the dibenzazepine backbone is shown to introduce stable planar chirality. This additional element of chirality gives rise to four possible isomers, and our synthesis of (*pS,R_S*)-**10** yields material of excellent enantiopurity. The synthetic methodology outlined here opens the possibility to tune sterics and electronics by modular combination of a variety of aryl-dibenzazepines (readily accessible by Suzuki cross coupling methodology from dibenzazepine)²³ with a range of well-known chiral sulfonates. The new ligands coordinate Rh(I) in a bidentate fashion and feature *sp*²–*sp*³ hybridization flexible azepine N atoms upon coordination. Even though the S–N functionality is rather pH-sensitive, preliminary catalysis results

show that preformed rhodium complexes **11** and **12** withstand the aqueous reaction conditions commanded by the Hayashi–Miyaura C–C coupling protocol and indeed operate also without base additives. However, the use of these ligands in aqueous solvent systems represents a potential source of erosion of enantioselectivity, and water-free protocols are currently being developed in our laboratory. Finally, planar chirality in ligand (*pS,R_S*)-**10** is found to be the overwhelming stereochemical factor defining the sense of chiral induction, and therefore diastereomeric forms such as (*pR,R_S*)-**10** represent worthwhile synthetic targets.

EXPERIMENTAL SECTION

Experiments involving sensitive compounds were carried out under anaerobic and anhydrous conditions, using standard Schlenk and glovebox techniques. Technical grade EtOAc, hexanes, and MeOH for flash column chromatography were purified by rotary evaporation. Solvents were distilled as follows: THF, Et₂O, and benzene from purple Na/Ph₂CO solutions; toluene from Na; pentane, C₆D₆, and THF-D₈ from Na₂K alloy; CH₃CN, CH₂Cl₂, and CD₂Cl₂ from CaH₂; NEt₃ and 1,4-dioxane from K. CD₃CN and CDCl₃ were degassed with three freeze–pump–thaw cycles and then kept in a glovebox over activated molecular sieves (3 and 4 Å, respectively). K₃PO₄ (99%, Aldrich) and diacetone-D-glucose (DAG, 98%, Carbosynth) were used as received. **5**,²³ (*S_S*)-**6**,^{18b} **8**,²³ PhLi,³³ (*R*)-**9**,¹⁸ [RhCl(COE)₂]₂,³⁴ were prepared according to published procedures. Elemental analyses (EA) were performed on a Euro EA 3000 analyzer, and air-sensitive samples were handled and prepared in a glovebox. NMR spectra were recorded on Jeol EX 270, ECP 400, or ECX 400 instruments operating at 269.71, 399.78, and 400.18 MHz for ¹H; 67.82, 100.52, and 100.62 MHz for ¹³C; and at 161.83 and 162.00 MHz for ³¹P, respectively. Chemical shifts are given in ppm and are reported relative to residual solvent peaks as secondary standard.³⁵ Delta NMR Processing and Control Software was used to process and visualize the NMR data.³⁶ HPLC was performed on a Shimadzu LC10 series instrument.

Synthesis of 10 wt % K₂CO₃-Impregnated Silica.²⁵ A 2 L round-bottomed flask was loaded with silica G60 (700 g) and K₂CO₃ (70 g). To this mixture MeOH (1.5 L) was added and then refluxed at 80 °C for 12 h while stirring. The solid was filtered off over a Büchner funnel, washed with MeOH (3 × 500 mL), and dried under vacuum at 40 °C for 48 h.

Improved Synthesis of Crystalline (*R*)-3-Deoxy-1,2:5,6-di-O-isopropylidene- α -D-glucopyranose-3-yl-*tert*-butanesulfinate ((*R_S*)-6**).**^{18b} To a cooled solution of *tert*-butanesulfinyl chloride (28.0 g, 199 mmol) in anhydrous THF (350 mL) at –78 °C was added dropwise Et₃N (21.1 g, 209 mmol) over 15 min followed by slow addition over 60 min of a solution of DMAP (4.86 g, 39.8 mmol) in THF (50 mL). The resulting mixture was stirred for 60 min at –78 °C, to which then a solution of diacetone glucose (25.9 g, 99.6 mmol) in THF (300 mL) was added dropwise over 7 h. The reaction mixture was stirred overnight and then quenched with HCl (10% aqueous). The mixture was extracted with CH₂Cl₂ (3 × 400 mL), and the organic phase washed with saturated aqueous NaHCO₃ and brine. After drying over Na₂SO₄ the volatiles were removed *in vacuo* to give products (*R_S*)-**6** and (*S_S*)-**6** (96:4 dr). This mixture was purified by column chromatography (hexane/diethyl ether, 9:1) and cooled to –5 °C to afford pure (*R_S*)-**6** as a white solid (35.2 g, 94%), which contained single crystals suitable for X-ray diffraction analysis. [α]_D²⁰ + 11.3 (*c* = 1.30, acetone). ¹H NMR (500 MHz, CDCl₃): δ = 5.89 (d, *J* = 3.5 Hz, 1 H), 4.81 (d, *J* = 3.57 Hz, 1 H), 4.69 (d, *J* = 2.3 Hz, 1 H), 4.16–4.13 (m, 3 H), 4.95–3.93 (m, 1 H), 1.50, 1.41 (2 s, 6 H), 1.30 (s, 6 H), 1.22 (s, 9 H) ppm. ¹³C{¹H} NMR (125 MHz, CDCl₃): δ = 112.3, 109.4, 105.3, 83.6, 82.6, 81.3, 71.8, 67.9, 58.5, 26.7, 26.2, 25.2, 21.5 ppm.

(*R*)-5-(*tert*-Butylsulfinyl)-5*H*-dibenzo[*b,f*]azepine ((*R*)-7**).** A deep blue solution of **5** (3.58 g, 18.0 mmol) in THF (40 mL) was cooled to –78 °C and then added dropwise to a stirred solution of (*R*)-**6** (5.95 g, 16.3 mmol) in THF (40 mL) at –78 °C. The

reaction mixture was allowed to rise slowly to 0 °C overnight and then was stirred another 48 h at this temperature. The volatiles were removed under reduced pressure, giving a brownish solid that was taken up in THF (100 mL) and K₂CO₃-silica-G60 (6 sp) and then stripped to an off-white powder. This mixture was subjected to flash column chromatography (K₂CO₃-silica-G60; *d* = 5 cm; *l* = 12 cm; EtOAc/*n*-hexane 1:9). Recrystallization from THF/*n*-pentane (1:5) afforded white crystals, which were recrystallized a second time from THF/*n*-pentane (1:3) and dried *in vacuo*. This procedure gives white crystals of excellent optical purity (3.33 g, 69%). ee = 99.3% by HPLC (column: Chiralpak AD-H; flow rate: 1 mL/min; *n*-hexane/*i*-PrOH = 95:5, *t* = 9.63 min, 11.04 min (major, (R)-isomer). [α]_D²⁰ = 105° (*c* = 1.0, in THF). EA: C, 72.85; H, 6.35; N, 4.73; S, 10.02; calcd for C₁₈H₁₉NOS: C, 72.69; H, 6.44; N, 4.71; S, 10.78. Mp = 118 °C. ¹H NMR (400 MHz, CDCl₃) δ 8.44 (d, *J* = 8 Hz, 1H), 7.91 (d, *J* = 8 Hz, 1H), 7.16–7.10 (m, 2H), 7.00–6.91 (m, 4H), 6.58–6.64 (m, 2H), 1.06 (s, 9H) ppm. ¹H NMR (400 MHz, CDCl₃) δ 7.90 (d, *J* = 8 Hz, 1H), 7.65 (d, *J* = 8 Hz, 1H), 7.38–7.21 (m, 2H), 7.20–7.17 (m, 4H), 6.82 (m, 2H), 1.00 (s, 9H) ppm. ¹³C{¹H} NMR (101 MHz, CDCl₃) δ 146.79, 142.74, 134.63, 131.70, 131.65, 130.28, 129.66, 129.41, 129.32, 129.19, 128.19, 127.03, 126.42, 125.81, 59.85, 24.06.

(S)-5-(tert-Butylsulfinyl)-5H-dibenzo[b,f]azepine ((S)-7). A deep blue solution of 5 (1.11 g, 5.58 mmol) in THF (20 mL) was cooled to –78 °C and then added dropwise to a stirred solution of (S)-6 (1.85 g, 5.08 mmol) in THF (20 mL) at –78 °C. The reaction mixture was allowed to rise slowly to 0 °C overnight and was then stirred another 48 h at this temperature. The volatiles were removed under reduced pressure, giving a brownish solid that was taken up in THF (100 mL) and K₂CO₃-silica-G60 (6 sp) and then stripped to an off-white powder. This mixture was subjected to flash column chromatography (K₂CO₃-silica-G60; *d* = 5 cm; *l* = 12 cm; EtOAc/*n*-hexane 1:9). Recrystallization from 1:3 THF/*n*-pentane afforded yellowish crystals, which were recrystallized a second time from 2:5 THF/*n*-pentane and dried *in vacuo*. This procedure gives white crystals of excellent optical purity (1.05 g, 70%). ee = 99.5% by HPLC (column: Chiralpak AD-H; flow rate: 1 mL/min; *n*-hexane/*i*-PrOH = 95:5, *t* = 8.90 min (major, (S)-isomer), 10.44 min. NMR spectra are identical to (R)-7.

rac-5-(tert-Butylsulfinyl)-5H-dibenzo[b,f]azepine (rac-7). A deep blue solution of 5 (500 mg, 2.59 mmol) in THF (20 mL) was added dropwise to a solution of phenyl-*tert*-butylsulfinate (428 mg, 2.16 mmol) in THF (40 mL) at –30 °C. The reaction mixture was allowed to reach RT over the course of 24 h. The volatiles were then removed under reduced pressure giving a brownish solid that was taken up in THF (30 mL) and K₂CO₃-silica (2 sp) and then stripped to an off-white powder. This mixture was subjected to flash column chromatography (K₂CO₃-silica; *d* = 5 cm; *l* = 12 cm; EtOAc/hexane 15:85) affording an off-white powder (487 mg, 76%). NMR spectra are identical with spectra of (R)-7 and (S)-7. HPLC conditions: Chiralpak AD-H; flow rate: 1 mL/min; *n*-hexane/*i*-PrOH = 95:5, *t* = 11.34 min, 12.99 min.

(pS,R_S)-5-(tert-Butylsulfinyl)-10-phenyl-5H-dibenzo[b,f]azepine ((pS,R_S)-10). A deep blue solution of 8 (1.411 g, 5.124 mmol) in THF (30 mL) was stirred for 1 h at 0 °C and then added dropwise to a stirred colorless solution of (R)-9 (1.99 g, 4.65 mmol) in THF (40 mL), which was kept at –78 °C. After completed addition, the temperature of the reaction mixture was allowed to rise slowly to RT overnight. The volatiles were then removed under vacuum to give a brownish solid, which was slurried in Et₂O (100 mL) for 4 h. The white solid was separated by filtration, dried, mixed with K₂CO₃-silica (6 sp) in THF (50 mL), and dried again. This mixture was subjected to flash column chromatography (K₂CO₃-silica; *d* = 5 cm; *l* = 15 cm; EtOAc/*n*-hexane = 1:9) affording white crystalline material (539 mg, 31%). Mp = 178 °C. EA: C 73.30, H 5.96, N 3.51, S 8.01; calcd for C₂₄H₂₃NOS·0.03CH₂Cl₂: C 73.15, H 5.96, N 3.51, S 8.04. [α]_D²⁰ = 50.4° (*c* = 1.00, THF). ee = 99.6% by HPLC (column: Chiralpak AD-H; flow rate: 1 mL/min; *n*-hexane/*i*-PrOH 95:5, *t* = 14.9 min (major), 19.6 min). ¹H NMR (400 MHz, CDCl₃) δ 7.97 (d, *J* = 7.9 Hz, 1H), 7.73 (d, *J* = 7.9 Hz, 1H), 7.43–7.26 (m, 9H), 7.17 (d, *J* = 7.3 Hz, 1H), 7.02 (d, *J* = 7.3 Hz, 1H), 1.07

(s, 9H) ppm. ¹³C{¹H} NMR (101 MHz, CDCl₃) δ 147.88, 143.96, 143.29, 135.99, 134.43, 130.44, 130.39, 130.00, 129.42, 129.05, 128.89, 128.44, 127.5, 127.38, 126.05, 59.83, 23.85 ppm.

rac-5-(tert-Butylsulfinyl)-10-phenyl-5H-dibenzo[b,f]azepine ((rac-10). A deep blue solution of 8 (650 mg, 2.36 mmol) in THF (20 mL) was added dropwise to a stirred solution of phenyl *tert*-butylsulfinate (428 mg, 2.15 mmol) in THF (40 mL), which was kept at –30 °C. The reaction mixture was allowed to slowly rise to RT over the course of 24 h. The mixture was quenched with water (30 mL), slurried for 0.5 h, the organic phase separated, and the aqueous phase extracted with EtOAc (3 × 15 mL). The combined organic phases were dried over MgSO₄, filtered, and stripped to a yellowish solid. Recrystallization in EtOAc/*n*-pentane yielded an off-white microcrystalline solid (237 mg, 41%). Enantioselective HPLC: see upper trace of Figure 3. The ¹H NMR (270 MHz, CDCl₃) spectrum shows a ca. 85:15 diastereomeric mixture of {(pS,S_S)-9 + (pR,R_S)-9}: {(pS,R_S)-9 + (pR,S_S)-9}: δ 8.00 (d, *J* = 8.1 Hz, 1H), 7.94 (d, *J* = 7.9 Hz, 1H), 7.72 (d, *J* = 7.9 Hz, 1H), 7.70 (d, *J* = 8.1 Hz, 1H), 7.50–6.90 (m, 22H), 1.13 (s, 9H, major diastereomer), 1.04 (s, 9H, minor diastereomer) ppm.

[RhCl((R)-7)]₂ ((S)-11). A solution of (R)-7 (640 mg, 2.15 mmol) in benzene (5 mL) was added dropwise to an orange slurry of [RhCl(coe)₂]₂ (772 mg, 1.07 mmol) in benzene (5 mL). The resulting deep-red solution was stirred for 15 h. Then, the volatiles were removed *in vacuo*, and the crude was slurried and washed with cold *n*-pentane (2 × 8 mL) and dried *in vacuo* to yield an orange powder (905 mg, 97%). EA: C 49.16, H 4.40, N 3.58; calcd for C₃₆H₃₈N₂O₂S₂Cl₂Rh₂: C 49.61, H 4.39, N 3.21. ¹H NMR (400 MHz, C₆D₆): δ 7.56 (d, 1H, ³J_{HH} = 7.6 Hz), 7.41 (d, 1H, ³J_{HH} = 7.6 Hz), 7.12–7.01 (3H, m), 6.84–6.75 (3H, m), 6.09 (d, 1H, ³J_{HH} = 9 Hz), 4.93 (d, 1H, ³J_{HH} = 9 Hz), 1.24 (9H, s) ppm. ¹³C{¹H} NMR (101 MHz, C₆D₆) δ 142.03, 140.69, 140.55, 138.83, 130.55, 130.08, 129.30, 129.31, 128.57, 129.93, 127.81, 127.69, 127.57, 127.45, 16.80, 126.35, 66.95, 65.82 (d, *J*_{C–Rh} = 15 Hz), 57.31 (d, *J*_{C–Rh} = 15 Hz), 24.76 ppm.

[RhCl((S)-7)]₂ ((R)-11). The same procedure as that for the synthesis of (S)-11 was followed. Spectroscopic data and yields correspond.

Single Crystals of rac-11. *rac*-11 was synthesized by analogy to (S)-11 (*vide supra*) by using the racemic ligand *rac*-7. Vapor diffusion of *n*-pentane into a filtered solution of *rac*-11 (60 mg) in CH₂Cl₂ (1.5 mL) afforded diffraction-quality single crystals.

[RhCl(pS,R_S)-10)]₂ ((S_N,S_S)-12). A solution of (pS,R_S)-10 (214 mg, 0.573 mmol) in benzene (3 mL) was added dropwise to an orange solution of [RhCl(coe)₂]₂ (206 mg, 0.287 mmol) in benzene (3 mL). The resulting dark red solution was stirred for 15 h, and then the volatiles were removed under HV. The crude solid was slurried and washed in cold pentane (2 × 5 mL) and dried *in vacuo* to afford an orange powder (270 mg, 92%). This analytically pure material is a 1:2 mixture of *cis/trans*-isomers. EA: C 56.28, H 4.59, N 2.44; calcd for C₄₈H₄₆N₂O₂S₂Cl₂Rh₂: C 56.32, H 4.53, N 2.74. ¹H NMR (400 MHz, C₆D₆) δ 8.84 (s, br, 2H, *trans*), 8.56 (s, br, 2H, *cis*), 7.55–6.95 (m, 20H), 6.85–6.70 (m, 4H), 5.62 (s, br, 2H, *cis*), 5.15 (s, br, 2H, *trans*), 1.61 (s, br, 18H, *cis*), 1.40 (s, br, 18H, *trans*) ppm. Recrystallization from C₆D₆ affords a microcrystalline precipitate in ca. 60% yield, which is the pure *trans*-isomer. Diffraction quality single crystals were obtained by layering a filtered solution of (S_N,S_S)-12 (20 mg) in C₆D₆ (0.6 mL) with *n*-hexane.

General Procedures for Rhodium-Catalyzed 1,4-Addition Reaction. Method A (Base-Free Protocol). In a glovebox, [RhCl(SO-alkene)]₂ (0.050 mmol), ArB(OH)₂ (1.50 mmol), and enone (1.00 mmol) were added to an oven-dried 20 mL scintillation vial equipped with a magnetic stir bar. Then, toluene (3.0 mL) and water (1.5 mL) were added and the vial sealed with a Teflon-lined screw cap. After stirring for 15 h at 40 °C the volatiles were removed *in vacuo* and the residue directly purified by flash chromatography (hexane/EtOAc 9:1) to afford the desired product as a colorless liquid. For spectroscopic data and determination of enantiomeric excesses, see the Supporting Information.

Method B (with K₃PO₄ Additive). In a glovebox, [RhCl(SO-alkene)]₂ (0.015 mmol), ArB(OH)₂ (1.50 mmol), and enone (1.00 mmol) were

added to an oven-dried 20 mL scintillation vial equipped with a magnetic stir bar. After adding 1,4-dioxane (3.0 mL) and water (1.0 mL) and stirring the mixture for 0.5 h, aqueous K_3PO_4 (1.0 M, 0.5 mL) was added by syringe to the vial. Stirring was then continued at 40 °C for 3 h, after which the reaction mixture was cooled to room temperature, quenched with water, and extracted with ethyl acetate (3 × 15 mL). The combined organic phases were dried over anhydrous $MgSO_4$, the volatiles evaporated, and the residue purified by flash chromatography (hexane/EtOAc 9:1) to afford the desired product as a colorless liquid. For spectroscopic data and determination of enantiomeric excesses, see the Supporting Information.

3-Phenyl-cyclohexanone (15aa).^{5c,37} Yield 98%, colorless oil, for 74.9% ee. 1H NMR (300 MHz, $CDCl_3$): δ 1.80–1.89 (m, 2H), 2.07–2.16 (m, 2H), 2.37–2.59 (m, 4H), 3.00–3.01 (m, 1H), 7.21–7.26 (m, 3H), 7.31–7.36 (m, 2H) ppm. ^{13}C NMR (75 MHz, $CDCl_3$): δ 25.4, 32.7, 41.1, 44.6, 48.8, 126.5, 126.6, 128.6, 144.3, 210.8 ppm. HPLC: Daicel Chiralpak OD-H, *n*-hexane/*i*PrOH = 98/2, 0.5 mL/min, 254 nm, t_R : 23.90 min ((*S*)-isomer), 25.59 min ((*R*)-isomer).

3-(4-Methylphenyl)cyclohexanone (15ab).^{5c,39} Yield 97%, white solid, 76% ee. 1H NMR (300 MHz, $CDCl_3$): δ 1.79–1.86 (m, 2H), 2.05–2.16 (m, 2H), 2.33 (s, 3H), 2.37–2.57 (m, 4H), 2.97–2.98 (m, 1H), 7.10–7.16 (m, 4H) ppm. ^{13}C NMR (75 MHz, $CDCl_3$): δ 20.9, 25.5, 32.9, 41.2, 44.3, 49.0, 126.4, 129.3, 136.2, 141.4, 211.1 ppm. HPLC: Daicel Chiralpak AD-H, *n*-hexane/*i*PrOH = 95/5, 0.7 mL/min, 254 nm, t_R : 9.14 min (major), 9.96 min.

3-(4-*tert*-Butylphenyl)cyclohexanone (15ac).^{5c} Yield 98%, white solid, 66% ee. 1H NMR (400 MHz, $CDCl_3$): δ 7.39 (d, J = 8.3 Hz, 2H), 7.19 (d, J = 8.3 Hz, 2H), 3.03 (tt, J = 11.7, 3.9 Hz, 1H), 2.66–2.39 (m, 4H), 2.22–2.08 (m, 2H), 1.92–1.75 (m, 2H), 1.35 (s, 9H). ^{13}C NMR (100 MHz, $CDCl_3$): δ 211.4, 149.5, 141.3, 126.2, 125.6, 49.0, 44.3, 41.3, 34.4, 32.8, 31.4, 25.6. HPLC: Daicel Chiralpak AS-H, *n*-hexane/*i*PrOH = 98/2, 0.6 mL/min, 254 nm, t_R : 18.60 min, 23.98 min (major).

3-(2-Naphthyl)cyclohexanone (15ad).³⁸ Yield 97%, white solid, 77% ee. 1H NMR (400 MHz, $CDCl_3$): δ 7.80 (dd, J = 8.7, 4.2 Hz, 3H), 7.63 (s, 1H), 7.50–7.41 (m, 2H), 7.35 (dd, J = 8.5, 1.7 Hz, 1H), 3.22–3.10 (m, 1H), 2.72–2.57 (m, 2H), 2.45 (dddd, J = 26.8, 19.6, 8.5, 3.8 Hz, 2H), 2.17 (tdd, J = 9.8, 6.9, 3.3 Hz, 2H), 2.01–1.73 (m, 2H). ^{13}C NMR (100 MHz, $CDCl_3$): δ 211.0, 141.8, 133.6, 132.4, 128.4, 127.7, 126.2, 125.7, 125.4, 124.8, 48.9, 44.8, 41.3, 32.7, 25.6. HPLC: Daicel Chiralpak AD-H Column, *n*-hexane/*i*PrOH = 98/2, 0.5 mL/min, 250 nm, t_R : 26.88 min, 29.12 min (major).

3-(4-Fluorophenyl)cyclohexanone (15ae).³⁹ Yield 95%, white solid, 70% ee. 1H NMR (300 MHz, $CDCl_3$): δ 1.77–1.85 (m, 2H), 2.05–2.17 (m, 2H), 2.38–2.56 (m, 4H), 2.98–3.00 (m, 1H), 6.98–7.04 (m, 2H), 7.15–7.20 (m, 2H). ^{13}C NMR (75 MHz, $CDCl_3$): δ 25.3, 32.8, 41.0, 43.9, 48.9, 115.3 (d, J = 21.1 Hz), 127.9 (d, J = 7.8 Hz), 140.0 (d, J = 3.2 Hz), 161.4 (d, J = 243.2 Hz), 210.6 ppm. HPLC: Daicel Chiralpak AD-H, *n*-hexane/*i*PrOH = 99/1, 1.0 mL/min, 254 nm, t_R : 27.51 min (major), 37.55 min.

3-(4-Methoxyphenyl)cyclohexanone (15af).⁴⁰ Yield 95%, yellowish solid, 68% ee. 1H NMR (300 MHz, $CDCl_3$): δ 1.76–1.83 (m, 2H), 2.03–2.15 (m, 2H), 2.35–2.55 (m, 4H), 2.95–2.96 (m, 1H), 3.79 (s, 3H), 6.86 (d, J = 8.6 Hz, 2H), 7.14 (d, J = 8.6 Hz, 2H) ppm. ^{13}C NMR (75 MHz, $CDCl_3$): δ 25.4, 32.9, 41.1, 43.9, 49.1, 55.2, 114.0, 127.4, 136.5, 158.2, 210.9 ppm. HPLC: Daicel Chiralpak OD-H, *n*-hexane/*i*PrOH = 98/2, 0.5 mL/min, 254 nm, t_R : 33.57 min (major), 35.60 min.

3-(3-Methoxyphenyl)cyclohexanone (15ag).^{5c} Yield 96%, colorless oil, 60% ee. 1H NMR (300 MHz, $CDCl_3$): δ 1.80–1.88 (m, 2H), 2.07–2.19 (m, 2H), 2.40–2.45 (m, 2H), 2.52–2.59 (m, 2H), 2.98–2.99 (m, 1H), 3.82 (s, 3H), 6.78–6.84 (m, 3H), 7.24–7.29 (m, 1H) ppm. ^{13}C NMR (75 MHz, $CDCl_3$): δ 18.5, 25.7, 34.2, 37.7, 41.9, 48.2, 104.6, 105.7, 111.9, 122.6, 139.0, 152.8, 203.9 ppm. HPLC: Daicel Chiralpak AD-H, *n*-hexane/*i*PrOH = 95/5, 1.0 mL/min, 254 nm, t_R : 9.26 min, 9.92 min (major).

3-(2-Methoxyphenyl)cyclohexanone (15ah).⁴¹ Yield 97%, colorless oil, 40% ee. 1H NMR (300 MHz, $CDCl_3$): δ 1.72–1.90 (m, 2H), 2.01–2.15 (m, 2H), 2.36–2.57 (m, 4H), 3.38–3.43 (m, 1H), 3.82 (s, 3H), 6.86–6.97 (m, 2H), 7.17–7.26 (m, 2H) ppm. ^{13}C NMR

(75 MHz, $CDCl_3$): δ 25.5, 30.9, 37.9, 41.3, 47.5, 55.2, 110.5, 120.6, 126.5, 127.5, 132.4, 156.7, 211.6 ppm. HPLC: Daicel Chiralpak AD-H, *n*-hexane/*i*PrOH = 96/4, 1.0 mL/min, 254 nm, t_R : 6.30 min, 7.44 min (major).

3-Phenylcyclopentanone (15ba).³⁹ Yield 98%, colorless oil, 69% ee. 1H NMR (300 MHz, $CDCl_3$): δ 1.98–2.02 (m, 1H), 2.30–2.49 (m, 4H), 2.62–2.71 (m, 1H), 3.40–3.48 (m, 1H), 7.23–7.28 (m, 3H), 7.34–7.38 (m, 2H) ppm. ^{13}C NMR (75 MHz, $CDCl_3$): δ 31.0, 38.7, 42.0, 45.6, 126.51, 126.54, 128.5, 142.9, 218.2 ppm. HPLC: Daicel Chiralpak, AS-H, *n*-hexane/*i*PrOH = 98/2, 0.7 mL/min, 254 nm, t_R : 27.03 min (major), 28.59 min.

3-(4-Methylphenyl)cyclopentanone (15bb).⁴² Yield 98%, colorless oil, 68% ee. 1H NMR (300 MHz, $CDCl_3$): δ 1.90–2.04 (m, 1H), 2.27–2.51 (m, 4H), 2.34 (s, 3H), 2.66 (dd, J = 18.0, 7.5 Hz, 1H), 3.33–3.45 (m, 1H), 7.16 (s, 4H). HPLC: Daicel Chiralpak AS-H, *n*-hexane/*i*PrOH = 90/10, 0.7 mL/min, 254 nm, t_R : 13.07 min (major), 13.99 min.

(+)-1,3-Diphenyl-3-(*para*-tolyl)propan-1-one (15cb).⁴³ Yield 98%, white solid, 36% ee. 1H NMR (300 MHz, $CDCl_3$): δ 2.30 (s, 3 H), 3.74 (d, J_{HH} = 7.2 Hz, 2 H), 4.82 (t, J_{HH} = 7.2 Hz, 1 H), 7.08–7.11 (m, 2 H), 7.15–7.22 (m, 3 H), 7.25–7.63 (m, 8 H), 7.94–7.96 (m, 2 H). ^{13}C NMR (75 MHz, $CDCl_3$): δ 20.9, 44.8, 45.6, 126.3, 127.7 (2 C), 127.8 (2 C), 128.0 (2 C), 128.5 (2 C), 129.3 (2 C), 133.0, 135.9, 137.1, 141.1, 144.4, 198.1. HPLC: Daicel Chiralcel AD-H, *n*-hexane/2-propanol = 98/2, 0.5 mL/min, 270 nm, t_R : 24.96 min, 29.87 min (major).

Crystallographic Information. CCDC-1845166 ((*R*)-6), CCDC-1845167 (*rac*-7), CCDC-1845168 ((*S,R*)-10), CCDC-1845169 (*rac*-11), and CCDC-1845170 ((*S,S*)-12) contain the supplementary crystallographic data for this paper. Collection and refinement parameters are summarized in Table S1.

■ ASSOCIATED CONTENT

Supporting Information

The Supporting Information is available free of charge on the ACS Publications website at DOI: 10.1021/acs.organomet.8b00591.

NMR spectra of ligands and complexes, HPLC traces of ligands (PDF)

Accession Codes

CCDC 1845166–1845170 contain the supplementary crystallographic data for this paper. These data can be obtained free of charge via www.ccdc.cam.ac.uk/data_request/cif, or by emailing data_request@ccdc.cam.ac.uk, or by contacting The Cambridge Crystallographic Data Centre, 12 Union Road, Cambridge CB2 1EZ, UK; fax: +44 1223 336033.

■ AUTHOR INFORMATION

Corresponding Author

*E-mail: romano.dorta@fau.de.

ORCID

Frank W. Heinemann: 0000-0002-9007-8404

Romano Dorta: 0000-0001-5986-9729

Notes

The authors declare no competing financial interest.

■ ACKNOWLEDGMENTS

We thank Ms. Christina Wronna for carrying out the elemental analyses and Ms. Cordula Ruppenstein and Mr. Rami Alahmar for performing catalytic tests. Financial support by Friedrich–Alexander University is acknowledged.

■ REFERENCES

(1) (a) Trost, B. M.; Rao, M. Development of Chiral Sulfoxide Ligands for Asymmetric Catalysis. *Angew. Chem., Int. Ed.* **2015**, *54*,

5026. (b) Sipos, G.; Drinkel, E.; Dorta, R. The emergence of sulfoxides as efficient ligands in transition metal catalysis. *Chem. Soc. Rev.* **2015**, *44*, 3834–3860. (c) Otocka, S.; Kwiatkowska, M.; Madalinska, L.; Kielbasinski, P. Chiral Organosulfur Ligands/Catalysts with a Stereogenic Sulfur Atom: Applications in Asymmetric Synthesis. *Chem. Rev.* **2017**, *117*, 4147–4181.

(2) Poater, A.; Ragone, F.; Mariz, R.; Dorta, R.; Cavallo, L. Comparing the Enantioselective Power of Steric and Electrostatic Effects in Transition-Metal-Catalyzed Asymmetric Synthesis. *Chem. - Eur. J.* **2010**, *16*, 14348–14353.

(3) The diastereomer of **3** is also readily accessible. Thaler, T.; Guo, L.-N.; Steib, A. K.; Raducan, M.; Karaghiosoff, K.; Mayer, P.; Knochel, P. Sulfoxide–Alkene Hybrids: A New Class of Chiral Ligands for the Hayashi–Miyaura Reaction. *Org. Lett.* **2011**, *13*, 3182–3185.

(4) (a) Feng, X.; Wang, Y.; Wei, B.; Yang, J.; Du, H. Simple N-Sulfinyl-Based Chiral Sulfur–Olefin Ligands for Rhodium-Catalyzed Asymmetric 1,4-Additions. *Org. Lett.* **2011**, *13*, 3300–3303. (b) Khiar, N.; Salvador, A.; Chelouan, A.; Alcudia, A.; Fernandez, I. Sulfolefin[†]: Highly modular mixed S/Olefin ligands for enantioselective Rh-catalyzed 1,4-addition. *Org. Biomol. Chem.* **2012**, *10*, 2366–2368. (c) Chen, G.; Gui, J.; Cao, P.; Liao, J. Chiral sulfoxide-olefin ligands: tunable stereoselectivity in Rh-catalyzed asymmetric 1,4-additions. *Tetrahedron* **2012**, *68*, 3220–3224. (d) Jin, S.-S.; Wang, H.; Zhu, T.-S.; Xu, M.-H. Design of N-cinnamyl sulfinamides as new sulfur-containing olefin ligands for asymmetric catalysis: achieving structural simplicity with a categorical linear framework. *Org. Biomol. Chem.* **2012**, *10*, 1764. (e) Wang, H.; Jiang, T.; Xu, M.-H. Simple Branched Sulfur–Olefins as Chiral Ligands for Rh-Catalyzed Asymmetric Arylation of Cyclic Ketimines: Highly Enantioselective Construction of Tetrasubstituted Carbon Stereocenters. *J. Am. Chem. Soc.* **2013**, *135*, 971–974. (f) Khiar, N.; Valdivia, V.; Salvador, A.; Chelouan, A.; Alcudia, A.; Fernández, I. *Adv. Synth. Catal.* **2013**, *355*, 1303. (g) Zhu, D.-X.; Chen, W.-W.; Xu, M.-H. Rhodium-catalyzed asymmetric intramolecular addition of arylboronic acids to ketones: catalytic enantioselective access to ³-hydroxy-^{2,3}-dihydrobenzofurans bearing a tetrasubstituted carbon stereocenter. *Tetrahedron* **2016**, *72*, 2637–2642. (h) Revu, O.; Uphade, M. B.; Prasad, K. R. Synthesis and evaluation of C₂-symmetric bis-sulfinamides as effective ligands in rhodium catalyzed addition of arylboronic acids to cycloalkenones. *Tetrahedron* **2016**, *72*, 5355–5362.

(5) (a) Defieber, C.; Ariger, M. A.; Moriel, P.; Carreira, E. M. Iridium-Catalyzed Synthesis of Primary Allylic Amines from Allylic Alcohols: Sulfamic Acid as Ammonia Equivalent. *Angew. Chem., Int. Ed.* **2007**, *46*, 3139–3143. For the structural authentication of **1**, see (b) Briceño, A.; Dorta, R. *cis*-Dichloridobis{[(S)-N-(3,5-dioxa-4-phosphacyclohepta[2,1-a;3,4-a']-dinaphthalen-4-yl)dibenz[*b,f*]azepin-κP}-palladium(II) deuteriochloroform disolvate. *Acta Crystallogr., Sect. E: Struct. Rep. Online* **2007**, *63*, m1718–m1719. For closely related variants of **1**, see (c) Mariz, R.; Briceño, A.; Dorta, R.; Dorta, R. Chiral Dibenzazepine-Based P-Alkene Ligands and Their Rhodium Complexes: Catalytic Asymmetric 1,4 Additions to Enones. *Organometallics* **2008**, *27*, 6605–6613. (d) Herrera, A.; Linden, A.; Heinemann, F.; Brachvogel, R.-C.; von Delius, M.; Dorta, R. Optimized Syntheses of Optically Pure P-Alkene Ligands; Crystal Structures of a Pair of P-Stereogenic Diastereomers. *Synthesis* **2016**, *48*, 1117–1123.

(6) [SH]dibenzo[*b,f*]azepine is an inexpensive building block for the synthesis of essential medicines, such as the anticonvulsant drug carbamazepine. Schindler, W.; New N-Heterocyclic Compounds, U.S. Patent 2,948,718A, 1960.

(7) For reviews on S(O)-alkene ligands, see (a) Dong, H.-Q.; Xu, M.-H.; Feng, C.-G.; Sun, X.-W.; Lin, G.-Q. Recent applications of chiral N-tert-butanesulfinyl imines, chiral diene ligands and chiral sulfur–olefin ligands in asymmetric synthesis. *Org. Chem. Front.* **2015**, *2*, 73. (b) Li, Y.; Xu, M.-H. Simple sulfur–olefins as new promising chiral ligands for asymmetric catalysis. *Chem. Commun.* **2014**, *50*, 3771. (c) Feng, X.; Du, H. Synthesis of Chiral Olefin Ligands and Their Application in Asymmetric Catalysis. *Asian J. Org. Chem.* **2012**, *1*, 204.

(8) Drinkel, E.; Briceño, A.; Dorta, R.; Dorta, R. Hemilabile P-Alkene Ligands in Chiral Rhodium and Copper Complexes: Catalytic Asymmetric 1,4 Additions to Enones. 2. *Organometallics* **2010**, *29*, 2503–2514.

(9) (a) Refs **5b–d**. (b) Linden, A.; Llovera, L.; Herrera, J.; Dorta, R.; Agrifoglio, G.; Dorta, R. “Chiral-at-Metal” Hemilabile Nickel Complexes with a Latent d¹⁰-ML₂ Configuration: Receiving Substrates with Open Arms. *Organometallics* **2012**, *31*, 6162–6171.

(10) Examples of chiral secondary aprotic sulfinamide ligands are rare. For a diaryl-sulfinamide, see (a) Yuan, S.; Zeng, Q.; Wang, J.; Zhou, L. Chiral N-aryl *tert*-butanesulfinamide-olefin ligands for rhodium-catalyzed asymmetric 1,4-addition of aryl boronic acids to cyclic enones. *ARKIVOC* **2017**, *2017*, 32–42. For aziridine derivatives, see (b) Chen, Q.; Chen, C.; Guo, F.; Xia, W. *Chem. Commun.* **2013**, *49*, 6433. For phosphorylated derivatives, see (c) Solà, J.; Revés, M.; Riera, A.; Verdager, X. N-Phosphino Sulfinamide Ligands: An Efficient Manner To Combine Sulfur Chirality and Phosphorus Coordination Behavior. *Angew. Chem., Int. Ed.* **2007**, *46*, 5020–5023. (d) Revés, M.; Achard, T.; Solà, J.; Riera, A.; Verdager, X. N-Phosphino-*p*-tolylsulfinamide Ligands: Synthesis, Stability, and Application to the Intermolecular Pauson-Khand Reaction. *J. Org. Chem.* **2008**, *73*, 7080–7087. (e) Benetskiy, E. B.; Bolm, C. Synthesis of phosphorylated sulfoximines and sulfinamides and their application as ligands in asymmetric metal catalysis. *Tetrahedron: Asymmetry* **2011**, *22*, 373–378. (f) Doran, S.; Achard, T.; Riera, A.; Verdager, X. Neutral vs. cationic rhodium (I) complexes of bulky N-phosphino sulfinamide ligands: Coordination modes and its influence in the asymmetric hydrogenation of Z-MAC. *J. Organomet. Chem.* **2012**, *717*, 135–140.

(11) Piras, E.; Läng, F.; Rüegger, H.; Stein, D.; Wörle, M.; Grützmacher, H. Chiral Phosphane Alkenes (PALs): Simple Synthesis, Applications in Catalysis, and Functional Hemilability. *Chem. - Eur. J.* **2006**, *12*, 5849–5858.

(12) (a) Hayashi, T.; Ueyama, K.; Tokunaga, N.; Yoshida, K. A Chiral Chelating Diene as a New Type of Chiral Ligand for Transition Metal Catalysts: Its Preparation and Use for the Rhodium-Catalyzed Asymmetric 1,4-Addition. *J. Am. Chem. Soc.* **2003**, *125*, 11508–11509. (b) Defieber, C.; Paquin, J.-F.; Serna, S.; Carreira, E. M. Chiral [2.2.2] Dienes as Ligands for Rh(I) in Conjugate Additions of Boronic Acids to a Wide Range of Acceptors. *Org. Lett.* **2004**, *6*, 3873–3876. (c) Paquin, J. F.; Stephenson, C. R. J.; Defieber, C.; Carreira, E. M. Catalytic Asymmetric Synthesis with Rh-Diene Complexes: 1,4-Addition of Arylboronic Acids to Unsaturated Esters. *Org. Lett.* **2005**, *7*, 3821–3824. (e) Paquin, J.-F.; Defieber, C.; Stephenson, C. R. J.; Carreira, E. M. Asymmetric Synthesis of 3,3-Diarylpropanals with Chiral Diene-Rhodium Catalysts. *J. Am. Chem. Soc.* **2005**, *127*, 10850. (f) Otomaru, Y.; Okamoto, K.; Shintani, R.; Hayashi, T. Preparation of C₂-Symmetric Bicyclo[2.2.2]octa-2,5-diene Ligands and Their Use for Rhodium-Catalyzed Asymmetric 1,4-Addition of Arylboronic Acids. *J. Org. Chem.* **2005**, *70*, 2503–2508. (g) Wang, Z.-Q.; Feng, C.-G.; Xu, M.-H.; Lin, G.-Q. Design of C₂-Symmetric Tetrahydropentalenes as New Chiral Diene Ligands for Highly Enantioselective Rh-Catalyzed Arylation of N-Tosylarylimines with Arylboronic Acids. *J. Am. Chem. Soc.* **2007**, *129*, 5336–5337. (h) Melcher, M.-C.; Ivisic, T.; Olagnon, C.; Tenten, C.; Lützen, A.; Strand, D. Control of Enantioselectivity in Rhodium(I) Catalysis by Planar Chiral Dibenzo[*a,e*]cyclooctatetraenes. *Chem. - Eur. J.* **2018**, *24*, 2344–2348.

(13) (a) Mariz, R.; Luan, X.; Gatti, M.; Linden, A.; Dorta, R. *J. Am. Chem. Soc.* **2008**, *130*, 2172–2173. (b) Burgi, J. J.; Mariz, R.; Gatti, M.; Drinkel, E.; Luan, X. J.; Blumentritt, S.; Linden, A.; Dorta, R. *Angew. Chem., Int. Ed.* **2009**, *48*, 2768. (c) Chen, J.; Chen, J.; Lang, F.; Zhang, X.; Cun, L.; Zhu, J.; Deng, J.; Liao, J. A C₂-Symmetric Chiral Bis-Sulfoxide Ligand in a Rhodium-Catalyzed Reaction: Asymmetric 1,4-Addition of Sodium Tetraarylborates to Chromenones. *J. Am. Chem. Soc.* **2010**, *132*, 4552–4553.

(14) See ref **7**, as well as (a) Chen, G.; Gui, J.; Li, L.; Liao, J. Chiral Sulfoxide-Olefin Ligands: Completely Switchable Stereoselectivity. *Angew. Chem., Int. Ed.* **2011**, *50*, 7681–7685. (b) Xue, F.; Li, X.; Wan, B. A Class of Benzene Backbone-Based Olefin–Sulfoxide Ligands for

Rh-Catalyzed Enantioselective Addition of Arylboronic Acids to Enones in Rhodium-Catalyzed Asymmetric Conjugate Additions. *J. Org. Chem.* **2011**, *76*, 7256–7262.

(15) (a) Sakai, M.; Hayashi, H.; Miyaura, N. Rhodium-Catalyzed Conjugate Addition of Aryl- or 1-Alkenylboronic Acids to Enones. *Organometallics* **1997**, *16*, 4229–4231. (b) Takaya, Y.; Ogasawara, M.; Hayashi, T.; Sakai, M.; Miyaura, M. Rhodium-Catalyzed Asymmetric 1,4-Addition of Aryl- and Alkenylboronic Acids to Enones. *J. Am. Chem. Soc.* **1998**, *120*, 5579–5580. (c) Takaya, Y.; Ogasawara, M.; Hayashi, T. Asymmetric 1,4-Addition of Phenylboronic Acid to 2-Cyclohexenone Catalyzed by Rh(I)/binap Complexes. *Chirality* **2000**, *12*, 469.

(16) (a) Lee, A.; Kim, K. Chiral Bicyclic Bridgehead Phosphoramidite (Briphos) Ligands for Asymmetric Rhodium-Catalyzed 1,2- and 1,4-Addition. *J. Org. Chem.* **2016**, *81*, 3520–3527. (b) Dou, X.; Lu, Y.; Hayashi, T. Base-Free Conditions for Rhodium-Catalyzed Asymmetric Arylation To Produce Stereochemically Labile α -Aryl Ketones. *Angew. Chem., Int. Ed.* **2016**, *55*, 6739–6743. (c) Miyamura, H.; Nishino, K.; Yasukawa, T.; Kobayashi, S. Rhodium-catalyzed asymmetric 1,4-addition reactions of aryl boronic acids with nitroalkenes: reaction mechanism and development of homogeneous and heterogeneous catalysts. *Chem. Sci.* **2017**, *8*, 8362–8372.

(17) Freitag, B.; Elsen, H.; Pahl, J.; Ballmann, B.; Herrera, A.; Dorta, R.; Harder, S. s-Block Metal Dibenzoazepinate Complexes: Evidence for Mg–Alkene Encapsulation. *Organometallics* **2017**, *36*, 1860–1866.

(18) (a) Khair, N.; Fernández, I.; Alcudia, F. Asymmetric synthesis of optically pure *tert*-butyl sulfoxides using the “DAG methodology. *Tetrahedron Lett.* **1994**, *35*, 5719–5722. (b) Chelouan, A.; Recio, R.; Alcudia, A.; Khair, N.; Fernández, I. DMAP-Catalyzed Sulfinylation of Diacetone-D-Glucose: Improved Method for the Synthesis of Enantiopure *tert*-Butyl Sulfoxides and *tert*-Butanesulfinamides. *Eur. J. Org. Chem.* **2014**, *2014*, 6935–6944.

(19) Harrowven, D. C.; Curran, D. P.; Kostiuk, S. L.; Wallis-Guy, I. L.; Whiting, S.; Stenning, K. J.; Tang, B.; Packard, E.; Nanson, L. Potassium carbonate–silica: a highly effective stationary phase for the chromatographic removal of organotin impurities. *Chem. Commun.* **2010**, *46*, 6335–6337.

(20) No racemization is observed in dry deoxygenated CDCl₃.

(21) García Ruano, J. L.; Parra, A.; Yuste, F.; Mastranzo, V. M. Mild and General Method for the Synthesis of Sulfonylamides. *Synthesis* **2008**, *2008*, 311–319.

(22) Efforts in our laboratory to obtain diffraction quality single crystals of enantiopure **7** are ongoing.

(23) Herrera, A.; Grasruck, A.; Heinemann, F.; Scheurer, A.; Chelouan, A.; Frieß, S.; Seidel, F.; Dorta, R. Developing P-Stereogenic, Planar–Chiral P-Alkene Ligands: Monodentate, Bidentate, and Double Agostic Coordination Modes on Ru(II). *Organometallics* **2017**, *36*, 714–720.

(24) The use of sulfinate **9** instead of **6** in this reaction is beneficial in terms of product purity and easier separation of the chiral auxiliary.

(25) The isolation of (p*R*,*R*_s)-**10** isomer in pure form is the subject of ongoing efforts in our laboratory.

(26) Sulfur is chosen as the lead atom. For the determination of descriptors of planar chirality, see for example Eliel, E. L.; Wilen, S. H. *Stereochemistry of Organic Compounds*; Wiley-Interscience, 1994; p 1121–1122.

(27) Traces have been generated sequentially under strictly identical conditions. For a trace of a representative sample with ee = 99.6% but with slightly differing retention time, see Figure S9.

(28) For the first DAG-derived sulfinates, see (a) Ridley, D. D.; Smal, M. A. Use of Carbohydrates in the Preparation of Optically Active Sulfoxides. *J. Chem. Soc., Chem. Commun.* **1981**, 505–506.

(b) Ridley, D. D.; Smal, M. A. Preparation of Arenesulfinic Esters of 1,2:5,6-Di-O-cyclohexylidene- α -D-glucopyranose, and Their Conversion into Optically Active Sulfoxides. *Aust. J. Chem.* **1982**, *35*, 495.

(c) Llera, J. M.; Fernández, I.; Alcudia, F. An efficient synthesis of both enantiomers of chiral non racemic methylsulfoxides from DAG. *Tetrahedron Lett.* **1991**, *32*, 7299–7302. For a structural report, see (d) Alayrac, C.; Saint-Clair, J.; Lemarié, M.; Metzner, P.; Averbuch-

Pouchot, M. 1,2:5,6-Di-O-isopropylidene- α -D-glucopyranosyl (S)-cyclohexanesulfinate. *Acta Crystallogr., Sect. C: Cryst. Struct. Commun.* **1999**, *55*, 262–264.

(29) The crystal structure of Lu-Senanayake sulfinate **9** is discussed in the following: Seidel, F.; Frieß, S.; Heinemann, F.; Chelouan, A.; Scheurer, A.; Grasruck, A.; Herrera, A.; Dorta, R. C₂-Symmetric (SO)N(SO) Sulfoxide Pincer Complexes of Mg and Pd: Helicity Switch by Ambidentate S/O-Coordination and Isolation of a Chiral Pd-Sulfinate. *Organometallics* **2018**, *37*, 1160–1171.

(30) (a) Dewar, M. J. S. *Bull. Chem. Soc. Fr.* **1951**, *18*, C71. (b) Chatt, J.; Duncanson, L. A. Olefin Co-ordination Compounds. Part III. * Infra-red Spectra and Structure: Attempted Preparation of Acetylene Complexes. *J. Chem. Soc.* **1953**, 2939–2947.

(31) For similar stereochemical models featuring S(O)-alkene ligands, see refs **3**, **4c**, **4d**, and **10b**.

(32) Falivene, L.; Credendino, R.; Poater, A.; Petta, A.; Serra, L.; Oliva, R.; Scarano, V.; Cavallo, L. SambVca 2. A Web Tool for Analyzing Catalytic Pockets with Topographic Steric Maps. *Organometallics* **2016**, *35*, 2286–2293.

(33) Schlosser, M.; Ladenberger, V. Notiz über die Darstellung reiner Lithiumaryle. *J. Organomet. Chem.* **1967**, *8*, 193–197.

(34) Van Der Ent, A.; Onderdelinden, A. L.; Schunn, R. A. *Inorg. Synth.* **2007**, *28*, 90–91.

(35) Fulmer, G. R.; Miller, A. J. M.; Sherden, N. H.; Gottlieb, H. E.; Nudelman, A.; Stoltz, B. M.; Bercaw, J. E.; Goldberg, K. I. *Organometallics* **2010**, *29*, 2176–2179.

(36) *Delta NMR Processing and Control Software*, version 4.3.6; JEOL USA, Inc.: Peabody, MA, 2006.

(37) Takaya, Y.; Ogasawara, M.; Hayashi, T.; Sakai, M.; Miyaura, N. Rhodium-Catalyzed Asymmetric 1,4-Addition of Aryl- and Alkenylboronic Acids to Enones. *J. Am. Chem. Soc.* **1998**, *120*, 5579–5580.

(38) Takaya, Y.; Ogasawara, M.; Hayashi, T. Rhodium-catalyzed asymmetric 1,4-addition of arylboron compounds generated in situ from aryl bromides. *Tetrahedron Lett.* **1999**, *40*, 6957–6961.

(39) Hayashi, T.; Takahashi, M.; Takaya, Y.; Ogasawara, M. Catalytic Cycle of Rhodium-Catalyzed Asymmetric 1,4-Addition of Organoboronic Acids. Arylrhodium, Oxa- π -allylrhodium, and Hydroxorhodium Intermediates. *J. Am. Chem. Soc.* **2002**, *124*, 5052–5058.

(40) Cho, C. S.; Motofusa, S.; Ohe, K.; Uemura, S.; Shim, S. C. A New Catalytic Activity of Antimony(III) Chloride in Palladium(0)-Catalyzed Conjugate Addition of Aromatics to α,β -Unsaturated Ketones and Aldehydes with Sodium Tetraphenylborate and Arylboronic Acids. *J. Org. Chem.* **1995**, *60*, 883–888.

(41) Boiteau, J.; Imbos, R.; Minnaard, A.; Feringa, B. Rhodium-Catalyzed Asymmetric Conjugate Additions of Boronic Acids Using Monodentate Phosphoramidite Ligands. *Org. Lett.* **2003**, *5*, 681–684.

(42) Feng, C.-G.; Wang, Z.-Q.; Tian, P.; Xu, M.-H.; Lin, G.-Q. Easily Accessible C₂-Symmetric Chiral Bicyclo[3.3.0] Dienes as Ligands for Rhodium-Catalyzed Asymmetric 1,4-Addition. *Chem. - Asian J.* **2008**, *3*, 1511–1516.

(43) Wong, J.; Gan, K.; Chen, H. J.; Pullarkat, S. A. Evaluation of Palladacycles as a Non-Rhodium Based Alternative for the Asymmetric Conjugate 1,4-Addition of Arylboronic Acids to α,β -Unsaturated Enones. *Adv. Synth. Catal.* **2014**, *356*, 3391–3400.